Elasticity, Viscosity, and Deformation of Orbital Fat

Ivo Schoemaker,[1,2] Pepijn P. W. Hoefnagel,[1,2] Tom J. Mastenbroek,[1] Cornelis F. Kolff,[1] Sander Schutte,[1] Frans C. T. van der Helm,[1] Stephen J. Picken,[3] Anton F. C. Gerritsen,[4] Piotr A. Wielopolski,[5] Henk Spekreijse,[6] and Huibert J. Simonsz[7]

PURPOSE. For development of a finite element analysis model of orbital mechanics, it was necessary to determine the material properties of orbital fat and its degree of deformation in eye rotation.

METHODS. Elasticity and viscosity of orbital fat of eight orbits of four calves and two orbits of one rhesus monkey were measured with a parallel-plate rheometer. The degree of deformation of orbital fat was studied in two human subjects by magnetic resonance imaging (MRI) through the optic nerve in seven (first subject) or fourteen positions of gaze from left to right. Bifurcations of veins in the fat were used as markers for displacement of the fat.

RESULTS. The elastic shear modulus (G') of calf orbital fat was between 250 Pa and 500 Pa, and of monkey orbital fat it was between 500 Pa and 900 Pa. The viscous shear modulus (G'') of calf orbital fat was between 80 Pa and 150 Pa, and for monkey orbital fat it was between 300 Pa and 500 Pa. In the MRI scans, it was found that markers in the fat, 1 to 5 mm posterior to the sclera, rotated with the eye for 36% to 53% of eye rotation; the remainder was accounted for by sliding of the eye within the Tenon capsule and within the orbital fat.

CONCLUSIONS. Elastic and viscous shear moduli of orbital fat are low. Little energy is dissipated in the fat. The required deformation of the fat during eye rotation is limited because the eye slides, to some extent, within the Tenon capsule. (*Invest Ophthalmol Vis Sci.* 2006;47:4819–4826) DOI:10.1167/iovs.05-1497

Little is known about the mechanical properties of orbital fat. Although it has been the subject of detailed anatomic studies, emphasis has been on the connective tissue septa encompassing the fat[1] and on the vasculature.[2] The supporting role of the fat has not been the subject of study, though the eye slides in and is supported by the orbital fat. During the development of a finite element analysis (FEA) model of the orbit,[3] the supporting role of the orbital fat proved to be very important, for instance in stabilizing rectus muscle paths.

In this FEA model, the geometry of the structures in the orbit, muscles, eye, fat, and bony orbit was determined, and these structures were divided into a mesh of tetrahedra. Material properties were assigned, and then deformations occurring during eye rotation—such as those caused by a contracting eye muscle—could be modeled. An FEA model of orbital mechanics has the great advantage of few preliminary assumptions. In a lumped model, the eye usually has three degrees of freedom (i.e., the eye rotates about a fixed point of rotation). In the FEA model of the orbit, the eye is supported by the orbital fat to outbalance the force of eye muscles pulling the eye into the orbit. Therefore, more accurate simulation of rotation in combination with translation of the eye is possible. Some cases of strabismus and orbital surgery can, hence, be modeled more accurately. One of the simulations performed with the FEA model was passive eye rotation about the line of sight,[3] imitating an experiment that had been performed previously in vivo.[4] In this simulation of passive rotation of the eye about the line of sight, the rectus muscle bellies remained in place, presumably because of their containment within the orbital fat; there were no explicit connections, such as pulley slings,[5] toward the orbital wall in the model. Stabilization of the muscle bellies occurred even when the elasticity of the orbital fat in the model was reduced to 200 Pa, a very low value. According to the active pulley hypothesis,[5] the muscle bellies are kept in place by pulleys. Pulley slings course toward the orbital wall anteriorly and act like springs to stabilize the rectus muscle paths in eye movements out of the plane of the muscle. The active pulley hypothesis has been questioned recently by demonstration of good eye motility in primates[6] and in a patient with severe Crouzon syndrome,[7] each of whom lacked (part of) the orbital wall. Recently, the functionality of the pulleys was questioned further in a histology study by McClung.[8]

In previous measurements of ocular mechanics, the stiffness of the fat and connective tissue surrounding the eye was measured indirectly by passive rotation of the eye itself, either during strabismus surgery after detachment of the medial and lateral rectus muscles or in awake volunteers without muscle detachment. Robinson et al.[9] and Collins et al.[10] found 0.48 g/deg eye rotation when the eye was rotated horizontally after detachment of the medial and lateral recti. In 29 awake volunteers, Collins et al.[11] found 1.05 g/deg, on average, when the eye was pulled nasally and 0.94 when the eye was pulled temporally, whereas the other eye fixated a target ahead and without muscle detachment. Barmack,[12] García et al.,[13] and Igarashi et al.[14] found similar values. In all these measurements, force was applied on a single point on the sclera, causing displacement of the center of the globe.[3]

In analyses of these previous measurements, no distinction has been made between elasticity of the fat and its encapsulating connective tissue, elasticity of the optic nerve, and sliding of the sclera within Tenon capsule. The latter component is important because less deformation of the orbital fat occurs during eye rotation if the sclera slides within Tenon capsule.

The elasticity and the viscosity of the orbital fat, together with its degree of deformation during eye rotation, constitute important parameters for the FEA model of the orbit but have not been measured previously. Therefore, we measured the

material properties of calf and monkey orbital fat and quantified the degree of deformation in two human subjects with MRI.

METHODS

We measured the elasticity and viscosity of orbital fat of both orbits of four calves and one rhesus monkey. We needed ample orbital fat to be able to perform the measurement with sufficient accuracy. Calf orbital fat was a convenient option. Calf orbit contains much fat, and a meat processing facility was close to the laboratory housing the appropriate measurement apparatus (this was important because the mechanical properties of fat change rapidly postmortem). The rhesus monkey was killed elsewhere for another study concerning the visual cortex. We also measured the elasticity and viscosity of kidney fat of the same animals for comparison: kidney fat has a dampening function and is not subjected to torsional deformation. All procedures were performed in compliance with the ARVO Statement for the Use of Animals in Ophthalmic and Vision Research.

Samples consisted of fat and its encapsulating connective tissue. These two components are inseparable. Measurement of the fat within the fat cells or its encapsulating connective tissue in isolation cannot be performed without destroying its structure and thereby its overall material properties. Moreover, these overall material properties provide the most useful data for the FEA model. The specimens of the orbital fat seemed homogeneous on macroscopic inspection.

Dynamic mechanical measurements were performed with a rheometer (ARES; TA Instruments, New Castle, DE) equipped with 100FRTN1 force transducer with a range of 0.004~100 g · cm torque and 0.1~100 g normal force, parallel-plate geometry. In the parallel-plate rheometer, the top plate is stationary and the bottom plate rotates in an oscillatory fashion at various frequencies. The torque generated during the oscillation is recorded, whereas the oscillation rate or frequency is decreased in stages. Rheological parameters of the tested material can be calculated using simple equations applied to the torque measured at the various frequencies. Because of the simple geometry of the shearing area, it is possible to express the results in fundamental units—Pa for elasticity and Pa · s for viscosity.

Some demands must be met when measuring with a parallel-plate rheometer. The measurements must be performed in the linear viscoelastic regime of the sample, the fat specimen should consist of one piece, and the entire surfaces of the upper and lower plates of the rheometer should be in good contact with the specimen. During our measurements we made sure these conditions were met as much as possible while taking into account the experimental constraints imposed by sample origin. The temperature of the plates was 37°C ± 1°C. The pressure exerted by the upper plate on the specimens during the measurements was approximately 500 Pa, which is near the estimated[15] and measured[16] orbital pressures of approximately 500 to 1000 Pa.

To determine the linear viscoelastic regime of the samples, a strain sweep at fixed frequency was performed before the actual measurements in a separate specimen. This showed that the viscoelasticity of orbital fat of calves and rhesus monkeys was linear from 0% to almost 130% deformation. Therefore, we chose to measure only at a deformation of 5% (ratio between excursion and height), thereby avoiding irreversible damage to the specimen caused by excessive deformation. Because we had first demonstrated that the viscoelasticity was linear up to 130% deformation, this was permissible. The strain sweep was made at one specific angular velocity; strain sweeps at different angular velocities gave no additional information.

During subsequent frequency sweeps, the lower plate was rotated sinusoidally at different angular velocities (ω), at fixed strain amplitude, in the linear regime. The experiments started with a maximal angular velocity of 100 rad/s, and this decreased stepwise to 0.1 rad/s over a period of 5.5 minutes. In a dynamic mechanical measurement, oscillatory shear strain (γ) was applied to the sample where $\gamma = \gamma_0 sin(\omega t)$.[17] The resultant stress was analyzed in terms of the elastic stress and the viscous dissipation using a storage modulus G', and a loss modulus G'', by: $\tau/\gamma_0 = G' sin(\omega t) + G'' cos(\omega t)$.[17] Here, τ was the measured dynamic stress. The first term in this expression was in phase with the applied strain and represented the elastic response of the material, as expressed by the elastic shear modulus G' (storage modulus). The second term was out of phase and attributed to viscous dissipation. It was related to the viscosity via $G'' = \eta\omega$,[17] where η was the viscosity. Because it was related to the viscous dissipation of energy, G'' was called the viscous shear modulus (loss modulus) of the material and depended on the viscosity and the speed of deformation.

The first series of measurements, in two sessions, were done on eight specimens of orbital fat derived from eight orbits of four calves. Calf heads were obtained immediately after slaughtering at a meat processing facility and were transported within half an hour to the laboratory in thermally insulated containers. Immediately before measurement, the orbital contents were removed by exenteration, whereby the skin was incised in a circular fashion down to the orbital rim and the periorbita was lifted from the walls of the bony orbit. The root of the resultant sac, deep in the orbit, was subsequently cut off, enabling the removal of the orbital contents in one piece. Each exenteration took approximately 5 minutes. From the orbital fat we took a large section, leaving its inner structure intact. This section was placed onto the lower circular plate ($d = 50$ mm) of the high-precision parallel-plate rheometer, and a second circular plate was lowered onto the specimen. Four measurements (first session) were performed with a circular top plate of $d = 50$ mm. The other four measurements (second session) were performed with a circular top plate of $d = 25$ mm because it was not always possible to cut a single piece of fat of 50 mm. The time between the end of the exenteration and the start of the measurement was less than 1 minute. Measurements were taken between 65 and 213 minutes postmortem.

The second series of measurements was performed on two specimens of orbital fat derived from the orbits from one rhesus monkey (*Macaca mulatta*, male, 8 years old). The orbital contents of the rhesus monkey were removed by exenteration approximately 10 minutes after death. After the exenteration, the orbital fat was put into a
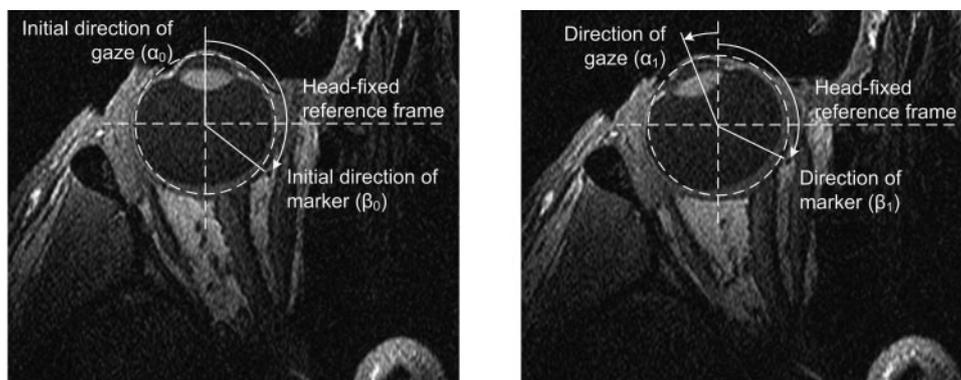

FIGURE 1. To assess the rotation of a marker in the orbital fat relative to the head in 7 (first subject) or 14 horizontal positions of gaze, the direction of gaze ($\alpha = \alpha_1 - \alpha_0$) relative to a head-fixed reference frame and the angle between the direction of the marker (β_1) and the head-fixed reference frame were used. The direction of the marker in approximate gaze ahead was taken as β_0. These two frames form part of Movie 1 (http://www.iovs.org/cgi/content/full/47/11/4819/DC1).

thermally insulated box of 37°C ± 2°C, with a humidity of 80%, and was transported to the laboratory. The time between the end of the exenteration and the start of the measurement was approximately 140 minutes.

From the same animals, specimens of kidney fat were taken. The specimen of kidney fat from the calves was transported to the laboratory in a manner similar to that for the calf heads. The specimen of kidney fat from the monkey was, however, not transported under controlled conditions and was desiccated on arrival. This specimen has been excluded.

MRI scans were made in 14 horizontal planes through the optic nerve of a human subject (24-year-old man) in seven horizontal posi-

tions of gaze. T_1-weighted, three-dimensional spoiled gradient echo scans (TR/TE/flip angle = 10.8/2.3ms/17°) were performed using a 1.5-T MRI scanner (General Electric Healthcare, Milwaukee, WI). Two 7.5-cm identification loops were located over both eyes for signal reception. Sequence parameters were adjusted accordingly to provide a scan time of approximately 1 minute per position per volume. The volume scan plane was adjusted using an initial localizer so that the center of the lens was aligned with the optic nerve at position 0 (resultant scan plane close to axial). Eyes were covered fully with 84 0.5-mm slices (interpolated by zero filling) with an in-plane resolution of 0.336×0.437 mm^2 pixels. An out-of-phase echo time (TE) of 2.3 milliseconds was selected to enhance the boundaries between water
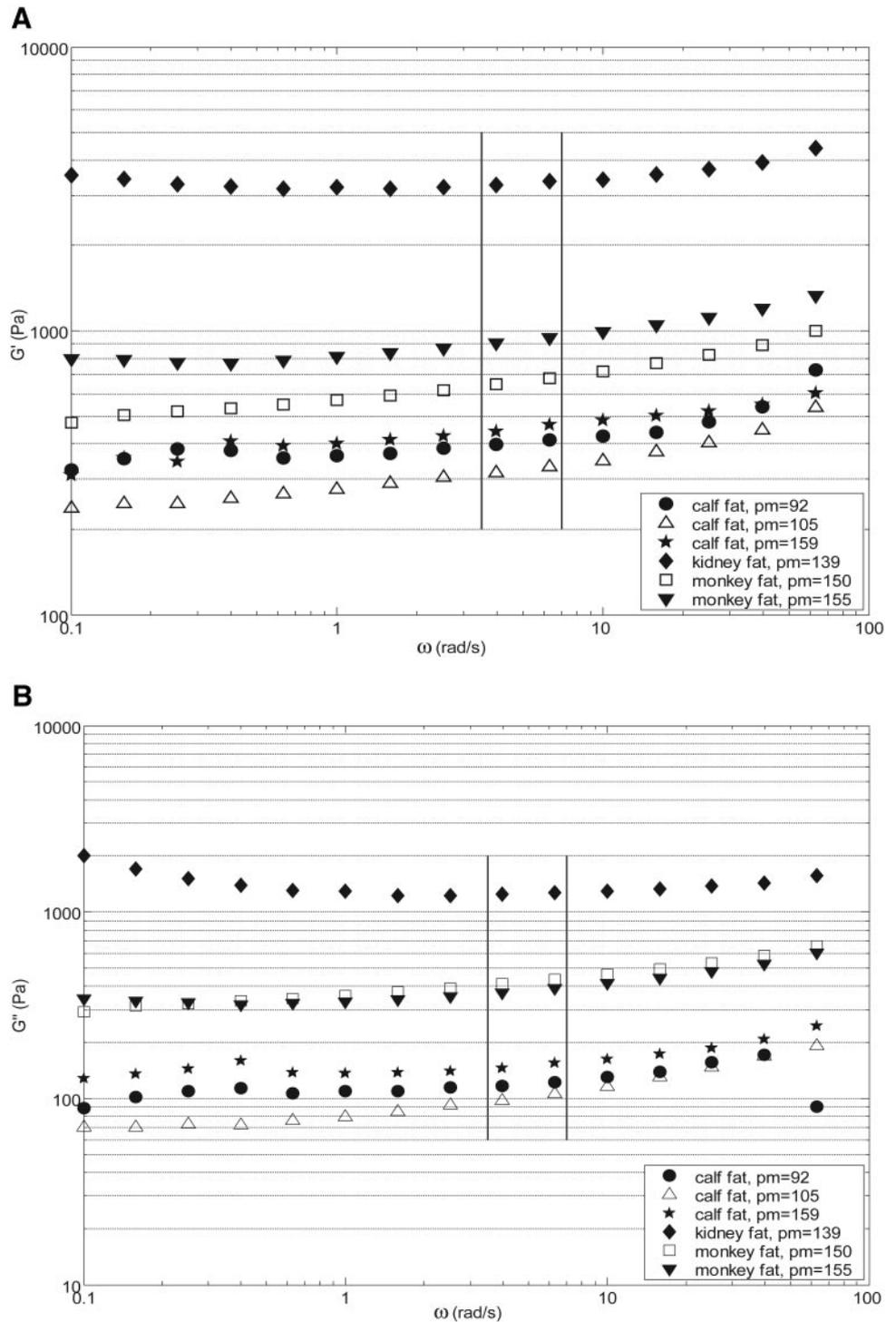

FIGURE 2. (**A**) Storage modulus (G', elasticity) and (**B**) loss modulus (G'', energy lost by viscous dissipation) of orbital fat of calves and a rhesus monkey. *Horizontal axis*: angular velocity (ω) in rad/s. *Vertical axis*: storage modulus (**A**) and loss modulus (**B**) expressed in pascals. Angular velocity (ω) increased from left to right, but measurements were actually performed with decreasing velocity: 10 rad/s was reached after 35 seconds, 1 rad/s was reached after 81 seconds. Identical symbols connect measurements of G' (**A**) and G'' (**B**) in one specimen. To illustrate the rate of deformation that occurred during eye movements, two *vertical bars* represent the approximate angular velocity occurring during 100 and 200 deg/s saccades, respectively, assuming that the fat immediately posterior to the sclera rotates with the eye for 50% of eye rotation. pm, postmortem period in minutes.
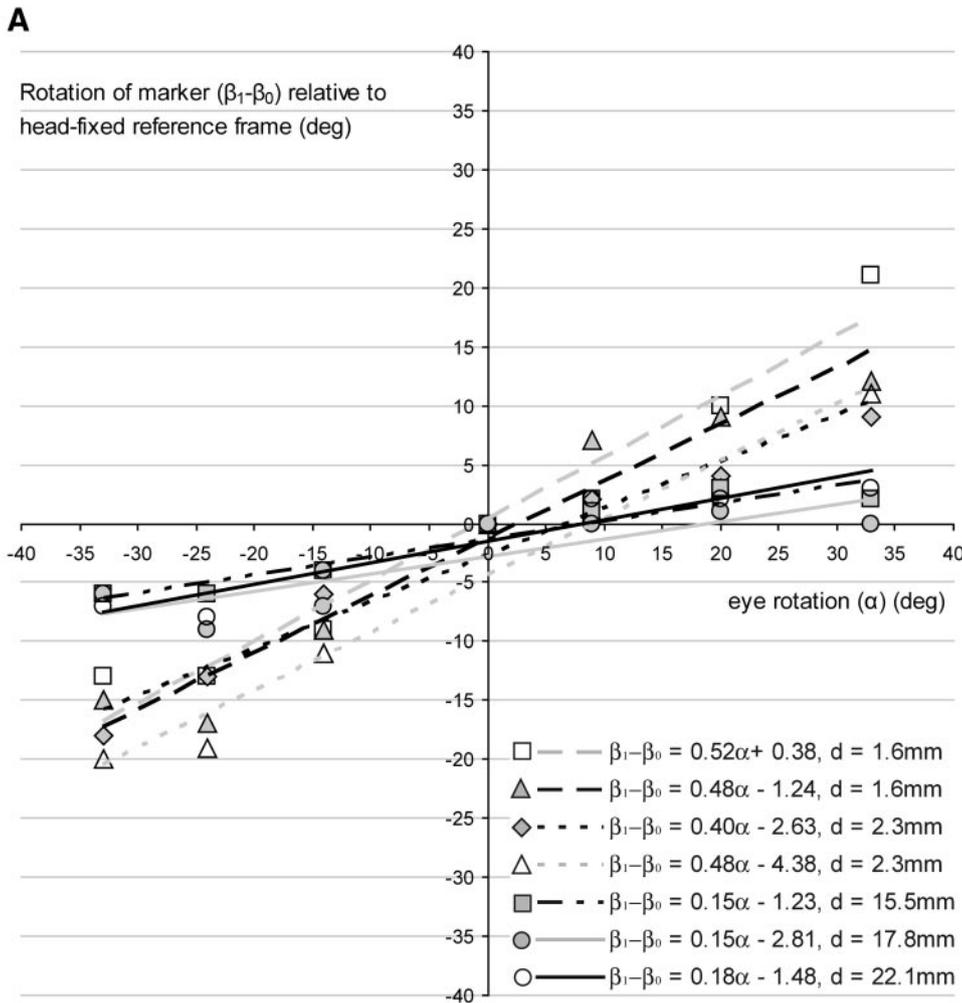
A

FIGURE 3. Rotation of markers of the fat behind the left eye (**A**) and the right eye (**B**) of the first subject and those behind the left eye of the second subject (**C**) in 7 (first subject) and 14 (second subject) positions of horizontal gaze. *Horizontal axis*: eye rotation ($\alpha = \alpha_1 - \alpha_0$, Fig. 1). *Vertical axis*: rotation of the marker relative to the head ($\beta_1 - \beta_0$, Fig. 1). The relative slope of the regression line, for each of the markers, was equal to the rotation of the marker ($\beta_1 - \beta_0$, Fig. 1) divided by the rotation of the eye itself (α, Fig. 1). Markers posterior in the orbit, 15 to 22 mm from the sclera, rotated with the eye for 7% to 18% of eye rotation. Markers near the globe, 1 to 5 mm from the sclera, rotated with the eye for 36% to 53% of eye rotation. d, distance of marker posterior to the sclera.

and fat (to aid boundary recognition, especially between vessels and fat).

An additional MRI scan was made through the optic nerve of another human subject (22-year-old woman) in 14 horizontal positions of gaze. T_1-weighted, three-dimensional spoiled gradient echo scans (TR/TE/flip angle = 8.1/1.9 ms/22°) were performed using a 3.0-T clinical MRI unit (General Electric Healthcare). Sequence parameters were adjusted accordingly to provide a scan time of approximately 1 minute per position per volume. The volume scan plane was adjusted with the use of an initial localizer so that the center of the lens was aligned with the optic nerve at position 0 (resultant scan plane close to axial). Eyes were covered fully with 128 0.4-m slices (interpolated by zero filling) with an in-plane resolution of 0.312 × 0.580 mm² pixels.

The head of each subject was fixated with sandbags and encircling tape around the forehead and the gantry of the MRI, limiting head movements. The range of head movement that did occur was subsequently found to be a limited head rotation about the vertical axis in a later MRI three-dimensional optical flow analysis. At the inside of the MRI, 7 (first subject) and 14 (second subject) fixation points were made on a horizontal line, corresponding with 7 and 14 horizontal positions of gaze. The center position of the fixation points corresponded with approximate gaze ahead.

Subjects did not always fixate with the same eye. Therefore, in the analysis, it was necessary to use the actual position of gaze of the eye as measured in the scans themselves. The horizontal line through the anterior margin of the two zygomal bones (first subject) or the horizontal line through the center of both eyes (second subject) was used as reference. In each scan, the direction of gaze was determined from

the line through the center of the globe and the center of the lens, relative to this reference.

Bifurcations of veins were used as markers for the displacement of the fat. Only bifurcations of veins that could be identified in the scans of all positions of gaze in equal planes were selected. Their respective points of bifurcation were then used as markers. Angular displacement of the marker from the center of the globe relative to the reference was measured in the scan (Fig. 1). This was repeated for each marker and for each of the positions of gaze.

RESULTS

Eight specimens were taken from eight orbits of four calves. Elastic shear modulus (G') was between 250 Pa and 500 Pa (Fig. 2A). Viscous shear modulus (G'') was between 80 and 170 Pa for the eight specimens (Fig. 2B). The four measurements of calf orbital fat were found to be very similar (Figs. 2A, 2B). For kidney fat of the same animals, the elastic shear modulus was between 3000 Pa and 5000 Pa, and the viscous shear modulus was between 1000 Pa and 2500 Pa. For the orbital fat of the rhesus monkey, higher values were between 500 Pa and 1050 Pa for elastic shear modulus and between 300 Pa and 700 Pa for viscous shear modulus.

Two possible measurement artifacts were encountered, one caused by too much water and the other caused by too little water. During the first calf session, only one of the four specimens was measured immediately after the orbital contents were taken from the orbit. The other three were kept for
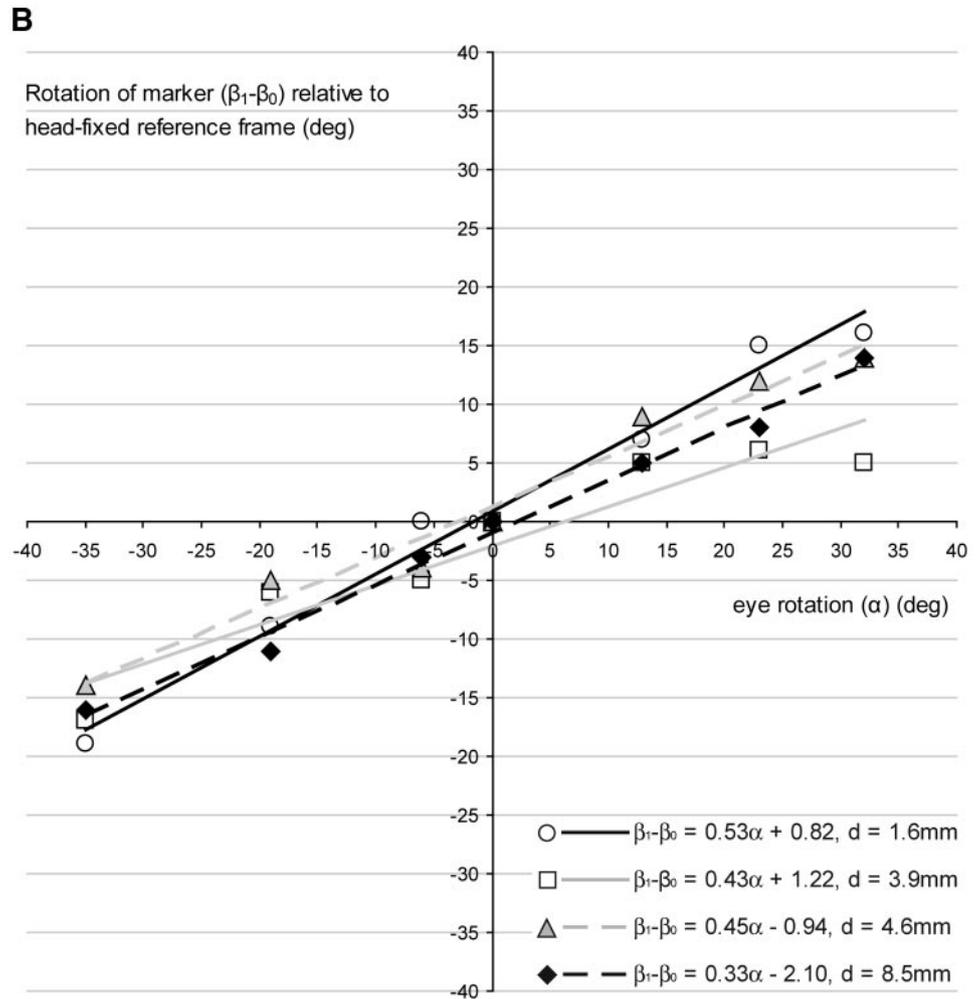
B

FIGURE 3. *(Continued)*

approximately 2 minutes in 0.9% NaCl to prevent desiccation. For these three specimens, conspicuously low values for storage modulus and loss modulus were found during the entire frequency sweeps at angular velocities from 100 rad/s to 0.1 rad/s over a period of 5.5 minutes. Apparently, the surplus of water worked as a lubricant. These specimens have been excluded.

During three of the five other measurements and during those in monkey fat, the edges of the fat, exposed to air during measurement, were kept moist by occasional sprinkling of a drop of 0.9% NaCl on the exposed surface of the edge. This was not done in the two remaining measurements, and G' and G'' increased considerably approximately 2 minutes after the measurements were begun. These specimens have also been excluded. The increase in G' and G'' might have been caused by desiccation; we noticed adhesion of the orbital fat to the plates on removal of the sample. Ophthalmic surgeons often see desiccation of exposed orbital fat during orbital surgery, and the desiccated fat may stick to the surgical drape. G' and G'' increased with increasing time intervals between death and exenteration, approximately 0.29 Pa/min for G' of calf orbital fat.

The actual horizontal positions of gaze of the first MRI scans were, for the right eye, 35°, 19°, and 6° (left gaze), 0° (reference), and 13°, 23°, and 32° (right gaze). For the left eye, they were 33°, 24°, and 14° (left gaze), 0° (reference), and 9°, 20°, and 33° (right gaze). The actual horizontal positions of gaze for the left eye in the second MRI scans were 37°, 30°, 24°, 20°,

15°, 8°, and 5° (left gaze), 0° (reference), and 6°, 10°, 14°, 24°, 28°, and 36° (right gaze).

In the first subject, 11 bifurcations, 4 behind the right eye and 7 behind the left eye, could be reliably identified in all 7 positions of gaze by meticulous comparison of the scans in equal planes. In the second subject, 3 bifurcations behind the left eye could be reliably identified in all 14 positions of gaze (Movie 1, available online at http://www.iovs.org/cgi/content/full/47/11/4819/DC1). These bifurcations were used as markers for the displacement of the fat relative to the head. In Figures 3A, 3B, and 3C, the rotation of these markers is plotted against rotation of the eye itself.

The rotation of the markers was almost proportional to rotation of the eye itself, allowing for linear data fitting. The slope of these linear fits represented the proportion that the marker rotated with the eye. For markers in the orbit 15 to 22 mm posterior to the sclera, the rotation of the markers was almost nil; they remained approximately stationary in the head. Movie 1 (http://www.iovs.org/cgi/content/full/47/11/4819/DC1) shows an overall impression of the deformation of the fat during eye movement, with arrows indicating the three markers used in the second subject.

Behind the left eye of the first subject, the proportions of rotation of the marker relative to the rotation of the eye were 52% (1.6 mm from the sclera), 48% (1.6 mm from the sclera), 40% (2.3 mm from the sclera), 48% (2.3 mm from the sclera), 15% (15.5 mm from the sclera), 15% (17.8 mm from the sclera), and 18% (22.1 mm from the sclera). Behind the right eye of the
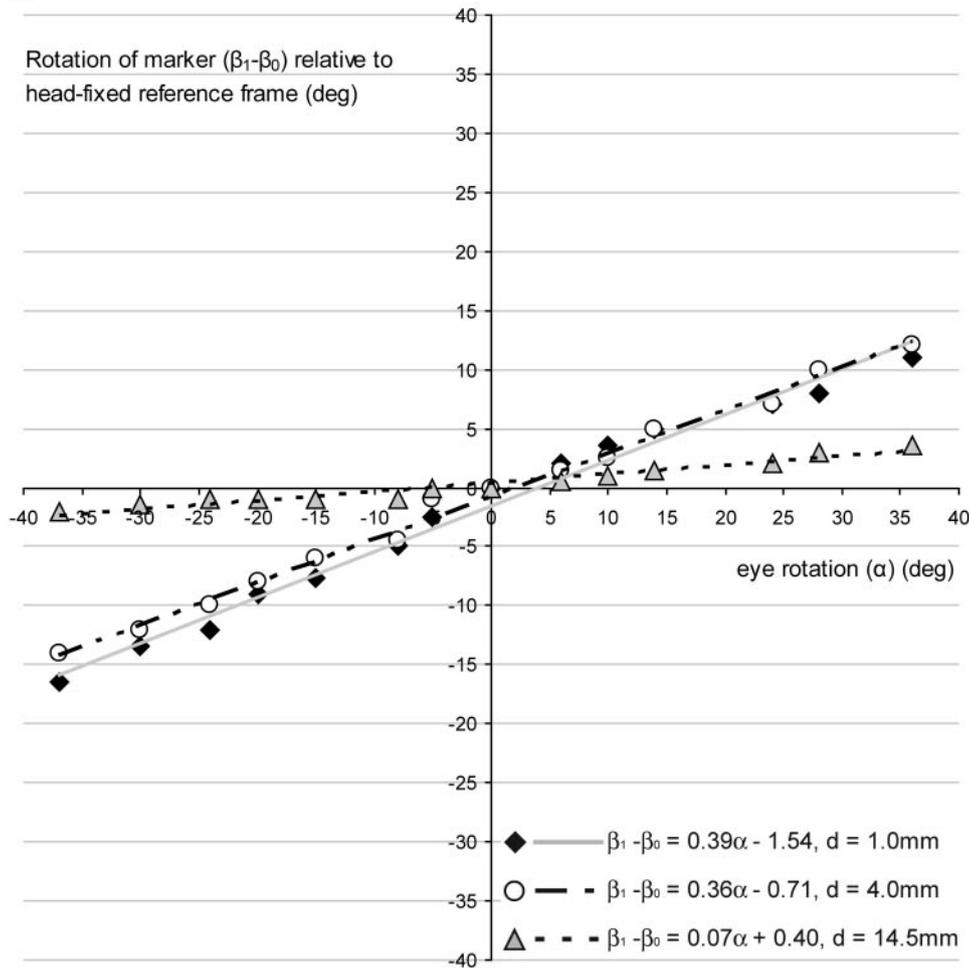
C

Rotation of marker (β_1-β_0) relative to head-fixed reference frame (deg)

eye rotation (α) (deg)

$\beta_1 - \beta_0 = 0.39\alpha - 1.54$, d = 1.0mm

$\beta_1 - \beta_0 = 0.36\alpha - 0.71$, d = 4.0mm

$\beta_1 - \beta_0 = 0.07\alpha + 0.40$, d = 14.5mm

FIGURE 3.   (*Continued*)

first subject, they were 53% (1.6 mm from the sclera), 43% (3.9 mm from the sclera), 45% (4.6 mm from the sclera), and 33% (8.5 mm from the sclera). For the markers behind the left eye of the second subject, the proportions of rotation of the marker relative to the rotation of the eye were 39% (1.0 mm from the sclera), 36% (4.0 mm from the sclera), and 7% (14.5 mm from the sclera). In Figure 4, these percentages are presented in relation to the distance of the markers from the sclera. Markers near the globe, 1 to 5 mm posterior to the sclera, rotated with the eye for 36% to 53% of eye rotation; the remainder was accounted for by sliding of the eye within Tenon capsule and within the orbital fat.

DISCUSSION

The elastic shear modulus (G') and viscous shear modulus (G'') of the orbital fat were low (Figs. 2A, 2B), and the G'' was low compared with the G'. To give an indication, its properties resembled those of a 10% solution of gelatin in water. When the viscous shear modulus, G'', is low, little energy is lost because of viscous dissipation during eye movements. We found higher values for G' and G'' in kidney fat, which has primarily a dampening function. For abdominal subcutaneous fat, a relatively low value (188.4 Pa) for G'' has also been found.[18] In histologic sections of the orbit,[1] the large size of the fat cells that, together with the encapsulating connective tissue septa, constitute the orbital fat, is conspicuous. In addi-

tion, the amount of connective tissue was low. These two anatomic properties might have helped to keep G' and G'' low.

The viscous shear modulus (G'' or energy lost by viscous dissipation) remains approximately the same with increasing angular velocity (ω) during sinusoidal deformation (Fig. 2B). As expressed by $G'' = \eta\omega$, the almost constant value of G'' implies that the viscosity (η) drops with increasing angular velocity (ω). In polymer mechanics, this phenomenon is called shear thinning. The shear thinning phenomenon has also been found for the viscoelasticity of human abdominal subcutaneous fat.[18] Decrease of viscosity with frequency has been found for the oculomotor plant.[19] Given that G' and G'' remained the same for different angular velocities, elasticity (G') and the viscous shear modulus (G'') can be treated as constants in future models of orbital mechanics.

Fuchs et al.[19] found stiffness of the oculomotor plant to increase with frequency. The stiffness in eye rotation may well be dominated by the behavior of the muscles, and their stiffness increases with increasing speed, whereas we found that stiffness of the orbital fat stayed constant with increasing velocity.

The full relevance of the values we found for elasticity and viscosity of the orbital fat for models of the oculomotor plant will be best demonstrated in the FEA model that we are currently developing.[3] Although the elasticity and viscosity of the fat were low, FEA model simulations showed that the fat can stabilize the muscle bellies in eye movement out of the plane of the muscle. In the FEA model, stabiliza-
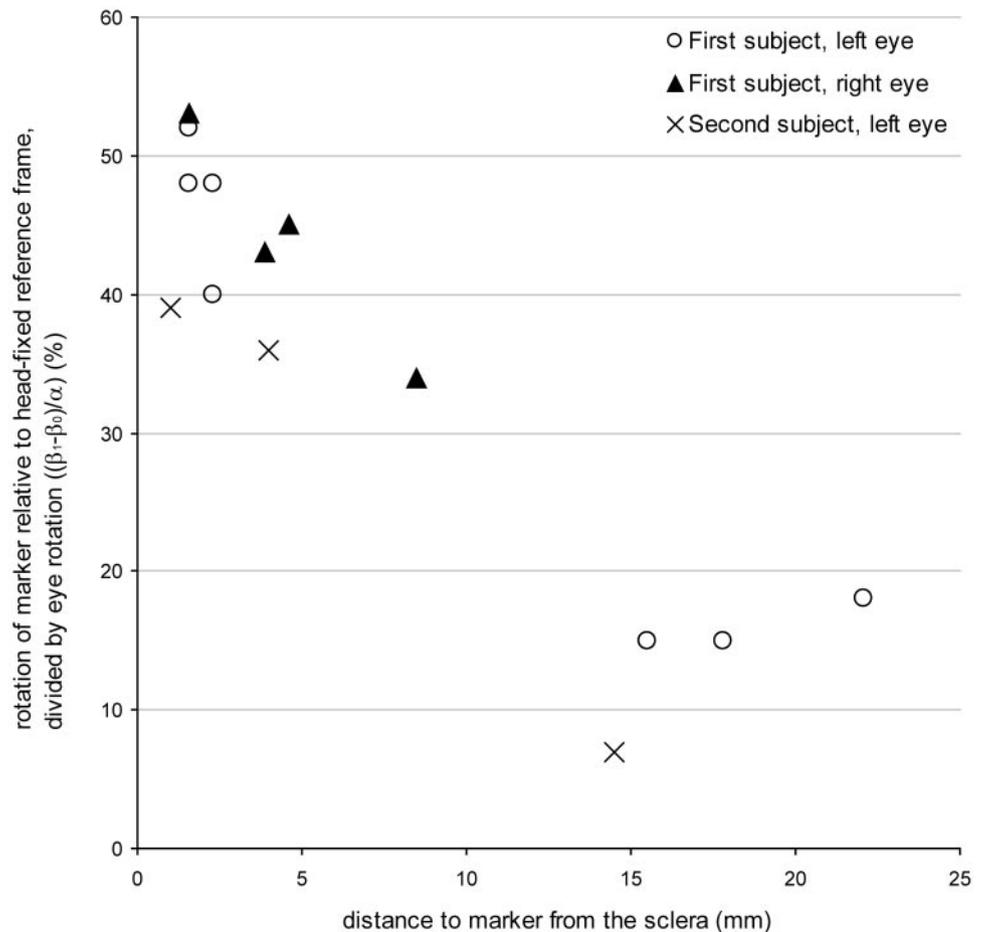
FIGURE 4. Rotation of the marker ($\beta_1 - \beta_0$, Fig. 1) divided by the rotation of the eye itself ($\alpha = \alpha_1 - \alpha_0$, Fig. 1) is presented here in relation to the distance of these markers from the sclera. Markers 15 to 22 mm from the sclera rotated with the eye for 7% to 18% of eye rotation. Markers 1 to 5 mm from the sclera rotated with the eye for 36% to 53% of eye rotation; the remainder was accounted for by sliding of the eye within Tenon capsule and within the orbital fat, respectively.

tion occurred even when the assumed elasticity of the fat was reduced to 200 Pa. Our measurements showed higher values, lending support to this prediction of the model. The necessity to invoke connective tissue bands between the orbital wall and the muscle belly for their stabilization[5] is thereby questionable. Nevertheless, the fat adjacent to the globe has a higher content of connective tissue, may be anisotropic, and may have unknown mechanical functions.

In previous analyses, no distinction was made between elasticity of the fat and sliding of the sclera within Tenon capsule. The latter component is important because less deformation of the orbital fat during eye rotation is needed if the sclera slides within Tenon capsule. With MRI in 7 (first subject) or 14 positions of gaze, we could determine the degree of deformation of the fat and, indirectly, the degree of sliding of the sclera within Tenon capsule and the orbital fat. Bergen[2] found that the veins in the orbit are suspended in the connective tissue septa,[1] whereas arteries perforate connective tissue septa. Therefore, we could reasonably assume that the movement of the veins represented the movement of the fat.

We found that markers in the fat in the posterior portion of the orbit, 15 to 22 mm posterior to the sclera, rotated with the eye for 7% to 18% of eye rotation. Markers 1 to 5 mm posterior to the sclera rotated with the eye for 36% to 53% of eye rotation; the remainder was accounted for by sliding of the eye within Tenon capsule and within the orbital fat. If the fat immediately posterior to the sclera followed approximately 50% of eye rotation and the fat posterior to the apex followed none, the elastic deformation of the orbital fat that took place when looking from 45° right to 45° left would be approximately 40%.

References

1. Koornneef L. *Spatial Aspects of Orbital Musculo-Fibrous Tissue in Man: A New Anatomical and Histological Approach.* Amsterdam: Swets & Zeitlinger; 1977.
2. Bergen MP. *Vascular Architecture of the Human Orbit.* Amsterdam: Swets & Zeitlinger; 1982.
3. Schutte S, van den Bedem SPW, van Keulen F, van der Helm FCT, Simonsz HJ. A finite-element analysis model of orbital biomechanics. *Vision Res.* 2006;11:1724–1731.
4. Simonsz HJ, Crone RA, de Waal BJ, Schooneman M, Lorentz de Haas HAL. Measurement of the mechanical stiffness in cyclotorsion of the human eye. *Vision Res.* 1984;24:961–968.
5. Demer JL. The orbital pulley system: a revolution in concepts of orbital anatomy. *Ann NY Acad Sci.* 2002;956:17–33.
6. Dimitrova DM, Shall MS, Goldberg SJ. Stimulation evoked eye movements with and without the lateral rectus muscle pulley. *J Neurophysiol.* 2003;90:3809–3815.
7. Van den Bedem SPW, Schutte S, Simonsz HJ. Mechanical properties and functional importance of pulley bands or 'faisseaux tendineux.' *Vision Res.* 2005;45:2710–2714.
8. McClung JR, Allman BL, Dimitrova DM, Goldberg SJ. Extraocular connective tissues: a role in human eye movements? *Invest Ophthalmol Vis Sci.* 2006;47:202–205.
9. Robinson DA, O'Meara DM, Scott AB, Collins CC. Mechanical components of human eye movements. *J Appl Physiol.* 1969;26:548–553.

10. Collins CC, Scott AB, O'Meara DM. Elements of the peripheral motor apparatus. *Am J Optom Arch Am Acad Optom.* 1969;46: 510–515.

11. Collins CC, Carlson MR, Scott AB, Jampolsky A. Extraocular muscle forces in normal human subjects. *Invest Ophthalmol Vis Sci.* 1981;20:652–664.

12. Barmack NH. Measurements of stiffness of extraocular muscles of the rabbit. *J Neurophysiol.* 1976;39:1009–1019.

13. García HA, Lavin JR, Massimino N, Ciancia AO. A new and practical model transducer forceps for measurement of active and passive forces in eye movements. *Binocular Vis.* 1987;2:69–76.

14. Igarashi Y, Takeda M, Sawa M. The study on mechanical properties of extraocular muscles in normal alert human subjects. *Sapporo Medical J.* 1985;54:569–581.

15. Simonsz HJ, Härting F, de Waal BJ, Verbeeten BWJM. Sideways displacement and curved path of recti eye muscles. *Arch Ophthalmol.* 1985;103:124–128.

16. Otto AJ. Volume discrepancies in the orbit and the effect on the intraorbital pressure. In: *Effects of Volume, Force and Pressure Alterations in the Orbit.* Amsterdam: Swets & Zeitlinger; 1991:53–66. Thesis.

17. Young RJ, Lovell PA. Mechanical properties. In: *Introduction to Polymers.* 2nd ed. London: Chapman & Hall. 1991:310–428.

18. Chan RW, Titze IR. Viscosities of implantable biomaterials in vocal fold augmentation surgery. *Laryngoscope.* 1998;108:725–731.

19. Fuchs AF, Scudder CA, Kaneko CR. Discharge patterns and recruitment order of identified motoneurons and internuclear neurons in the monkey abducens nucleus. *J Neurophysiol.* 1988;60:1874–1895.